WIMP search by the DAMA experiment at Gran Sasso

P. Belli

Dip.to di Fisica, Università di Roma "Tor Vergata"
and INFN, sez. Roma2, I-00133 Rome, Italy

and

R. Bernabei[a], M. Amato[b], F. Cappella[a], R. Cerulli[a], C.J. Dai[c], H.L. He[c], G. Ignesti[b], A. Incicchitti[b], H.H. Kuang[c], J.M. Ma[c], F. Montecchia[a], F. Nozzoli[a], D. Prosperi[b] [1]

[a] *Dip.to di Fisica, Università di Roma "Tor Vergata"*
and INFN, sez. Roma2, I-00133 Rome, Italy,
[b] *Dip.to di Fisica, Università di Roma "La Sapienza"*
and INFN, sez. Roma, I-00185 Rome, Italy,
[c] *IHEP, Chinese Academy, P.O. Box 918/3, Beijing 100039, China.*

DAMA is searching for rare processes by developing and using several kinds of radiopure scintillators: in particular, NaI(Tl), liquid Xenon and CaF_2(Eu). The main results are here summarized with particular attention to the investigation of the WIMP annual modulation signature.

PRESENTED AT

COSMO-01
Rovaniemi, Finland,
August 29 – September 4, 2001

[1] Neutron measurements in collaboration with: M. Angelone, P. Batistoni, M.Pillon (ENEA, C.R. Frascati P.O. Box 65, I-00044 Frascati, Italy). Some of the results on rare processes in collaboration with: V. Yu. Denisov, V. I. Tretyak, O.A. Ponkratenko, Yu. G. Zdesenko (Institute for Nuclear Research, MSP 03680 Kiev, Ukraine).

1 Introduction

DAMA is devoted to the search for rare processes by developing and using low radioactivity scintillators. Its main aim is the search for relic particles (WIMPs: Weakly Interacting Massive Particles). In addition, due to the radiopurity of the used detectors and of the installations, several searches for other possible rare processes are also carried out, such as e.g. on exotics, on $\beta\beta$ processes, on charge-non-conserving processes, on Pauli exclusion principle violating processes, on nucleon instability and on solar axions[1, 2, 3, 4, 5, 6, 7, 8, 9, 10, 11, 12, 13].

The main experimental set-ups running at present are: the $\simeq$ 100 kg NaI(Tl) set-up, the $\simeq$ 6.5 kg liquid Xenon (LXe) set-up and the so-called "R&D" apparatus. Moreover, a low-background germanium detector is operative underground for measurements and selections of sample materials.

In the following the most recent results achieved with the $\simeq$ 6.5 kg LXe set-up and with the "R&D" apparatus will be briefly recalled, while a more dedicated discussion will be devoted to the present results on the investigation of the WIMP annual modulation signature by the $\simeq$ 100 kg NaI(Tl) set-up.

2 The LXe experiment

We pointed out the interest in using liquid Xenon as target-detector for particle dark matter search deep underground since ref. [14]. Several prototypes were built and related results published [15]. The final choice was to realize a pure liquid Xe scintillator directly collecting the emitted UV light and filled with Kr-free Xenon gas isotopically enriched. The detailed description of this set-up and of its performances have been described in ref. [16]. Kr-free Xenon enriched in ^{129}Xe at 99.5% has been used since time, while more recently the set-up has been modified in order to run alternatively either with this gas or with Kr-free Xenon enriched in ^{136}Xe at 68.8%.

After preliminary measurements both on elastic and inelastic WIMP-^{129}Xe scattering [17, 18], the recoil/electron light ratio and the pulse shape discrimination capability in a similar pure LXe scintillator have been measured both with Am-B neutron source and with 14 MeV neutron generator [19]. After some upgrading of the set-up, new results on the WIMP search have been obtained [19, 20]. In particular, in ref. [19] the pulse shape discrimination in pure LXe scintillators has been exploited (see Fig. 1). Moreover, in 2000/2001 further measurements on the recoil/electron light ratio with 2.5 MeV neutron generator have been carried out at ENEA-Frascati; see ref. [21] for details and comparisons. Fig. 2 summarizes the measured values. The inelastic excitation of ^{129}Xe by Dark Matter particles with spin-dependent coupling has also been searched for preliminarily in ref. [18] and, more recently, in ref. [20].

Other rare processes have been investigated by filling the detector with the Kr-free Xenon gas enriched in ^{129}Xe at 99.5%.

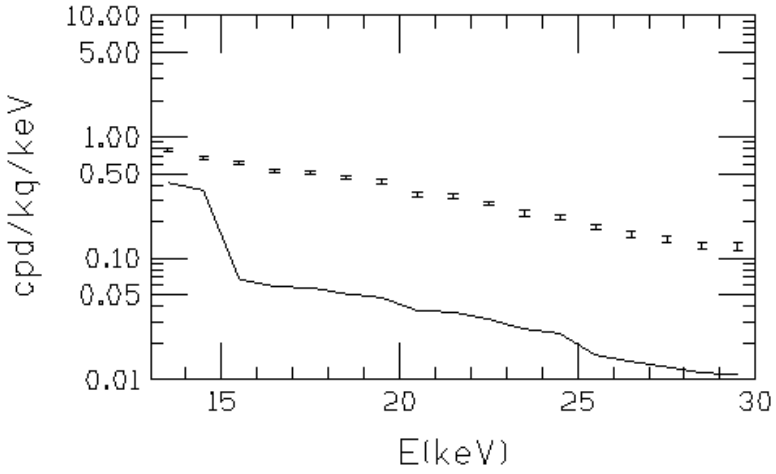

Figure 1: Low energy distribution (statistics of 1763.2 $kg \times day$) measured with the vessel filled with ^{129}Xe; the continuous line represents the upper limits at 90% C.L. obtained for the recoil fractions [19].

In particular, as regards the electron stability, limits on the lifetime of the electron decay in both the disappearance and the $\nu_e + \gamma$ channels were set in ref. [1]. The limits on the lifetime of the latter channel has been more recently improved to: $2.0(3.4) \cdot 10^{26}$

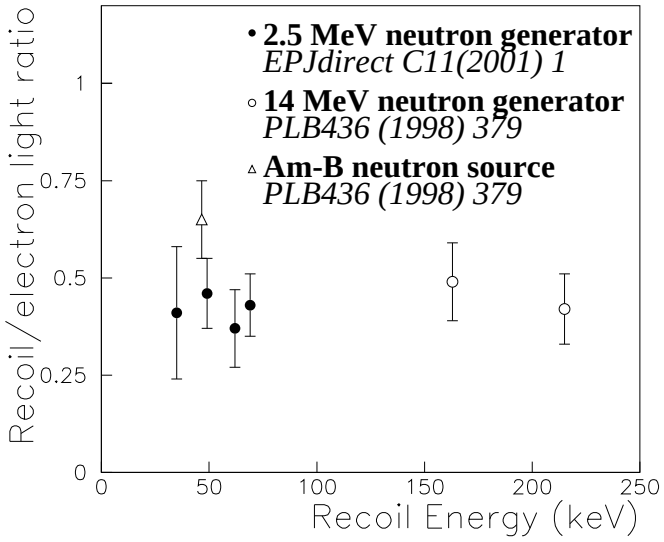

Figure 2: Measured behaviour of the recoil/electron light ratio with recoil energy. Note that the energy of the data point of AmB neutron source is an average which refers also to much lower energies than those explored with the 2.5 MeV neutrons.

y at 90% (68%) C.L. [10]. Furthermore, new lifetime limits on the charge non-conserving electron capture with excitation of ^{129}Xe nuclear levels have been established to be in the range $(1-4)\cdot 10^{24}$ y at 90% C.L. for the different excited levels of ^{129}Xe [9]. The most stringent restrictions on the relative strengths of charge non-conserving processes have been derived: $\epsilon_W^2 < 2.2\times 10^{-26}$ and $\epsilon_\gamma^2 < 1.3\times 10^{-42}$ at 90% C.L.

Moreover, the nucleon and di-nucleon decay into invisible channels [11] has been investigated by searching for the radioactive daughter nuclei, created after the nucleon or di-nucleon disappearance in the parent nuclei. This new approach has the advantage of a branching ratio close to 1 and – if the parent and daughter nuclei are located in the detector itself – also an efficiency close to 1. The obtained limits at 90% C.L. are: $\tau(p \rightarrow$ invisible channel$) > 1.9\cdot 10^{24}$ y; $\tau(pp \rightarrow$ invisible channel$) > 5.5\cdot 10^{23}$ y and $\tau(nn \rightarrow$ invisible channel$) > 1.2\cdot 10^{25}$ y. These limits are similar or better than those previously available; the limits for the di-nucleon decay in $\nu_\tau\bar{\nu}_\tau$ have been set for the first time; moreover, the limits are valid for every possible disappearance channel [11].

Finally as mentioned above, more recently the set-up has been modified to allow the use of Kr-free Xenon enriched in ^{136}Xe at 68.8%. Preliminary measurements have been carried out during 6843.8 hours [13] and new experimental limits have been obtained for $\beta\beta$ decay processes in ^{136}Xe, improving those previously available by factors ranging between 1.5 and 65. In particular, for the 3 possible channels without neutrinos the following half life limits (90% C.L.) have been achieved: $7.0\cdot 10^{23}$ y for the channel $\beta\beta$ $0\nu(0^+ \rightarrow 0^+)$; $4.2\cdot 10^{23}$ y for the channel $\beta\beta$ $0\nu(0^+ \rightarrow 2^+)$; $8.9\cdot 10^{22}$ y for the channel $\beta\beta$ $0\nu M(0^+ \rightarrow 0^+)$. For comparison, we note that the obtained experimental limits on the half life of the process $\beta\beta$ $0\nu(0^+ \rightarrow 0^+)$ is lower only than the one obtained for the case of ^{76}Ge. Moreover, the limits (90% C.L.) on the channels $\beta\beta$ $2\nu(0^+ \rightarrow 0^+)$ $1.1\cdot 10^{22}$ y and $\beta\beta$ $0\nu M(0^+ \rightarrow 0^+)$ are at present the most stringent ones not only for the ^{136}Xe isotopes, but also for every kind of nucleus investigated so far either by active or by passive source method. Furthermore, upper bounds on the effective neutrino mass have been set considering various theoretical models for the evaluation of the elements of the nuclear matrix; they vary between 1.5 eV and 2.2 eV (90% C.L.). Finally, in the framework of the same models we have also obtained upper limits on the effective coupling constant Majoron - neutrino; they range in the interval: $4.8\cdot 10^{-5}$ and $7.1\cdot 10^{-5}$ (90% C.L.).

In conclusion, competitive results have been achieved by the DAMA LXe set-up by using Kr-free isotopically enriched Xenon gas. Further upgradings to improve the detector performance are under consideration, while the data taking is continuing with both enrichments.

3 Results from the "R&D" set-up

The "R&D" set-up is used to measure the performances of prototype detectors and to perform small scale experiments. In particular, several experiments on the investigation of $\beta\beta$ decay processes in ^{136}Ce, ^{142}Ce, ^{40}Ca, ^{46}Ca, ^{48}Ca, ^{130}Ba, ^{106}Cd [2, 4, 5, 6] (see Fig.

3); other measurements are in progress and/or in preparation.

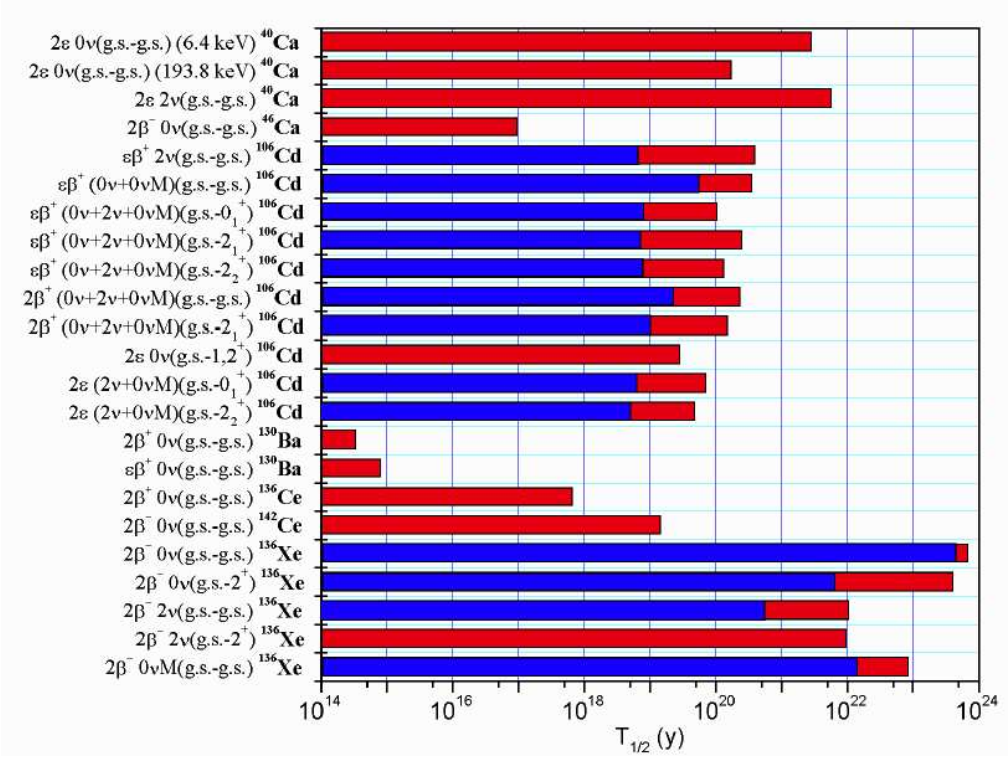

Figure 3: Light gray: experimental limits on the half-life of several $\beta\beta$-decay-candidate isotopes investigated by DAMA (90% C.L. with exception of the results on Barium and Cerium isotopes, which are at 68% C.L.) [2, 4, 5, 6]. Dark gray: previous best experimental limits (90% C.L.).

4 Results from the $\simeq$ 100 kg NaI(Tl) set-up

The $\simeq$ 100 kg NaI(Tl) DAMA set-up allows us to explore several kinds of rare processes regarding WIMPs, processes forbidden by Pauli exclusion principle, exotics, charge non conserving processes and solar axions[3, 7, 8, 12, 22, 23, 24, 25, 26, 27, 28, 29]. A full description of the apparatus and its performances can be found in ref.[25].

Let us preliminarily briefly summarize recent results – not referred to the WIMP search – obtained by means of this set-up.

A search for processes normally forbidden by the Pauli exclusion principle was carried out and an improved limit for spontaneous emission rate of protons in ^{23}Na and ^{127}I has been determined. In particular, the upper limit on the unit time probability of non-paulian emission of protons with energy $E_p \geq 10$ MeV is 4.6×10^{-33} s^{-1} and the corresponding lower limit on the mean life results 0.7×10^{25} y for ^{23}Na and 0.9×10^{25} y for ^{127}I [3].

The same set-up has allowed to set a new limit on the electron stability by considering for the first time the "disappearance" channel of L-shell electrons in Iodine. With a statistics of 19511 $kg \times day$ we have obtained: $\tau > 4.2 \times 10^{24}$ y (68% C.L.) for the process $e^- \rightarrow 3\nu, majoron + \nu$ or anything invisible [8].

Furthermore, new lifetime limits have been obtained on the charge non-conserving electron capture with excitation of ^{127}I and ^{23}Na nuclear levels. By analysing a statistics of 34866 $kg \times day$, limits in the range: $(1.5 - 2.4) \times 10^{23}$ y (up to two orders of magnitude higher than the ones previously available) have been obtained; also stringent restrictions on the relative strengths of the charge non-conserving (CNC) processes have been set [7].

Competing results have also been achieved by searching for neutral SIMPs: neutral particles with masses between few GeV and the GUT scale and cross sections on protons up to 10^{-22} cm^2, embedded in the galactic halo ($\beta \simeq 10^{-3}$). Although their large cross section, the neutral SIMPs interaction rate should be relatively low because of their low density in the galactic halo. Two "planes" of NaI(Tl) in the $\simeq$ 100 kg NaI(Tl) DAMA set-up have been used for this search, excluding neutral SIMPs with masses up to 4×10^{16} GeV [24]. With the same set-up also a new limit has been set on the neutral nuclearites (a possible new form of matter containing roughly equal number of up, down and strange quarks.). The model independent upper limit at 90% C.L. on the neutral nuclearites flux is: $\Phi < 1.9 \times 10^{-11}$ s^{-1}cm^{-2}sr^{-1} [24].

Recently this set-up has also allowed to set a new limit on solar axions by exploiting the Primakoff effect in NaI crystals. Analysing a statistics of 53437 $kg \times day$ the limit $g_{a\gamma\gamma} < 1.7 \times 10^{-9}$ GeV^{-1} (90% C.L.) [12] has been obtained (see Fig. 4); the region with axion mass greater than 0.03 eV (not accessible by other direct methods) has been explored and KSVZ axions with mass greater than 4.6 eV have been excluded at 90 % C.L. (see Fig. 4).

As regards the WIMP search, the recoil/electron light ratio and the pulse shape discrimination capability have been measured by neutron source and competitive results have been achieved on the WIMP-nucleus elastic scattering by exploiting the pulse shape discrimination technique in ref. [22]. Moreover, studies on the possible diurnal variation of the low energy rate in the data collected by the $\simeq$ 100 kg NaI(Tl) have been carried out. We recall that a diurnal variation of the low energy rate in WIMP direct searches can be expected because of the Earth's daily rotation. In fact, during the sidereal day the Earth shields a given detector with a variable thickness, eclipsing the "wind" of Dark Matter particles but only in case of high cross section candidates (to which small halo fraction would correspond). By analyzing a statistics of 14962 $kg \times day$ no evidence of diurnal rate variation with sidereal time has been observed [23]; this result supports that the effect pointed out by the studies on the WIMP annual modulation signature (see later) would account for a halo fraction $\gtrsim 10^{-3}$.

Let us note that the highly radiopure $\simeq$ 100 kg NaI(Tl) set-up has been originally developed to investigate the WIMP annual modulation signature, thus the remaining part of this paper will be devoted to summarize the present results on this topics.

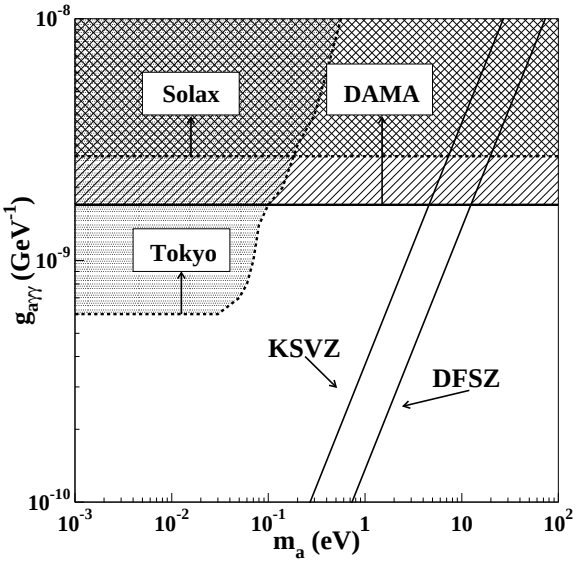

Figure 4: Exclusion plot for the axion coupling constant, $g_{a\gamma\gamma}$, versus the axion mass, m_a. The limit achieved by this experiment is shown together with theoretical expectations and previous direct searches for solar axions[12].

5 Investigation of the WIMP annual modulation signature

The WIMPs are embedded in the galactic halo; thus our solar system, which is moving with respect to the galactic system, is continuously hit by a WIMP "wind". The quantitative study of such "wind" allows both to obtain information on the Universe evolution and to investigate Physics beyond the Standard Model. The WIMPs are mainly searched for by elastic scattering on target nuclei, which constitute a scintillation detector. In particular, the $\simeq$ 100 kg NaI(Tl) set-up [25] has been realized to investigate the so-called WIMP "annual modulation signature". In fact, since the Earth rotates around the Sun, which is moving with respect to the galactic system, it would be crossed by a larger WIMP flux in June (when its rotational velocity is summed to the one of the solar system with respect to the Galaxy) and by a smaller one in December (when the two velocities are subtracted). The fractional difference between the maximum and the minimum of the rate is expected to be of order of $\simeq 7\%$. The $\simeq$ 100 kg highly radiopure NaI(Tl) DAMA set-up [25] can effectively exploit such a signature because of its well known technology, of its high intrinsic radiopurity, of its mass, of the deep underground experimental site and of its suitable control of the operational parameters. The annual modulation signature is very distinctive as we have already pointed out [25, 26, 27, 28, 29, 30, 31, 32]. In fact, a WIMP-induced seasonal effect must simultaneously satisfy all the following requirements: the rate must contain a component modulated according to a cosine function (1) with one year period (2) and a phase that peaks around $\simeq 2^{nd}$ June (3); this modulation must be

found in a well-defined low energy range, where WIMP induced recoils can be present (4); it must apply to those events in which just one detector of many actually "fires", since the WIMP multi-scattering probability is negligible (5); the modulation amplitude in the region of maximal sensitivity must be $\lesssim$7% (6). Only systematic effects able to fulfil these 6 requirements could fake this signature; therefore for some other effect to mimic such a signal is highly unlikely.

Here the results obtained by analysing the data of four annual cycles investigating the annual modulation signature by means of the $\simeq$ 100 kg NaI(Tl) set-up are summarized (see Table 1). Cumulative analyses of a total statistics of 57986 $kg \times day$ have been carried

Table 1: Released data sets [22, 26, 27, 28, 29, 31, 32].

period	statistics ($kg \times day$)
DAMA/NAI-1	4549
DAMA/NaI-2	14962
DAMA/NaI-3	22455
DAMA/NaI-4	16020
Total statistics	57986
+ DAMA/NaI-0	upper limit on recoils by PSD

out [29, 30, 31] properly including the physical constraint which arises from the measured upper limit on the recoil rate [22, 30]. Both model independent and model dependent analyses have been performed. We remark that various uncertainties exist in every model dependent calculations concerning WIMP direct detection search (the same is for exclusion plot as well as for allowed regions in the WIMP-proton cross section versus WIMP mass plane). They are present on some general features such as e.g. the real behaviour of the WIMP velocity distribution (which we have considered so far isothermal and Maxwellian), on the adopted particle model and on the values taken for all the parameters needed in the calculations.

6 Annual modulation signature and related studies

6.1 Model independent analysis

A model independent analysis of the data of the four annual cycles offers an immediate evidence of the presence of an annual modulation of the rate of the single hit events in the lowest energy interval (2 – 6 keV) as shown in Fig. 5. There each data point has been obtained from the raw rate measured in the corresponding time interval, after subtracting the constant part.

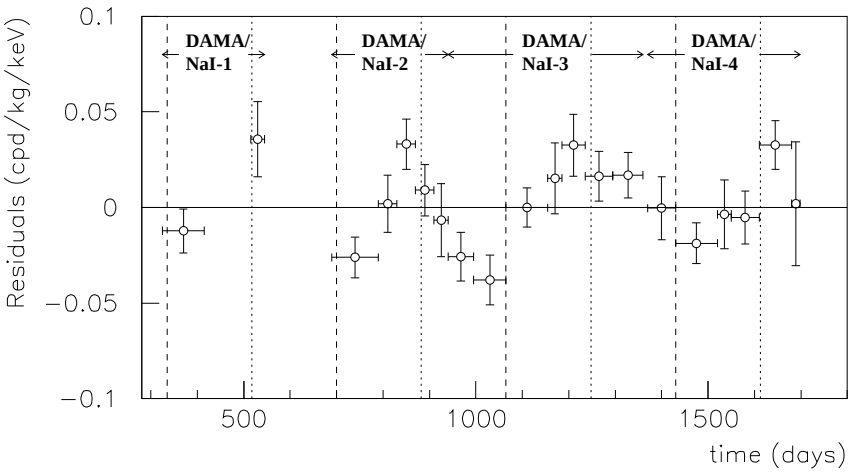

Figure 5: Model independent residual rate for single hit events, in the 2–6 keV cumulative energy interval, as a function of the time elapsed since January 1-st of the first year of data taking. The expected behaviour of a WIMP signal is a cosine function with minimum roughly at the dashed vertical lines and with maximum roughly at the dotted ones.

The χ^2 test on the data of Fig. 5 disfavors the hypothesis of unmodulated behaviour (probability: $4 \cdot 10^{-4}$), while fitting these residuals with the function $A \cdot \cos\omega(t - t_0)$, one gets: i) for the period $T = \frac{2\pi}{\omega} = (1.00 \pm 0.01)$ year when t_0 is fixed at the 152.5^{th} day of the year (corresponding to $\simeq$ 2 June); ii) for the phase $t_0 = (144 \pm 13)$ days, when T is fixed at 1 year. In the two cases A is: (0.022 ± 0.005) cpd/kg/keV and (0.023 ± 0.005) cpd/kg/keV, respectively.

We have extensively discussed the results of the investigations of the known sources of possible systematics when releasing the data of each annual cycle; moreover, a dedicated paper [30] has been released on possible systematics, where in particular the data of the DAMA/NaI-3 and DAMA/NaI-4 running periods have been considered in quantitative evaluations. No known systematic effect or side reaction able to mimic a WIMP induced effect has been found as discussed in details in ref. [30].

In conclusion, a WIMP contribution to the measured rate is candidate by the result of the model independent approach independently on the nature and coupling with ordinary matter of the possible WIMP particle.

6.2 Model dependent analyses

To investigate the nature and coupling with ordinary matter of a possible candidate, a suitable energy and time correlation analysis is necessary as well as a complete model framework. We remark that a model framework is identified not only by general astro-

physical, nuclear and particle physics assumptions, but also by the set of values used for all the parameters needed in the model itself and in related quantities (for example WIMP local velocity, v_0, form factor parameters, etc.).

At present the lightest supersymmetric particle named neutralino is considered the best candidate for WIMP. In supersymmetric theories both the squark and the Higgs bosons exchanges give contribution to the coherent (SI) part of the neutralino cross section, while the squark and the Z^0 exchanges give contribution to the spin dependent (SD) one. Note, in particular, that the results of the data analyses [29, 31, 32] summarized here and in the following hold for the neutralino, but are not restricted only to this candidate.

The differential energy distribution of the recoil nuclei in WIMP-nucleus elastic scattering can be calculated [22, 33] by means of the differential cross section of the WIMP-nucleus elastic processes

$$\frac{d\sigma}{dE_R}(v, E_R) = \left(\frac{d\sigma}{dE_R}\right)_{SI} + \left(\frac{d\sigma}{dE_R}\right)_{SD} \quad (1)$$

where v is the WIMP velocity in the laboratory frame and E_R is the recoil energy.

In the following, the results obtained by analysing the data in some of the possible model frameworks are summarized.

I. WIMPs with dominant SI interaction in a given model framework

Often the spin-independent interaction with ordinary matter is assumed to be dominant since e.g. most of the used target-nuclei are practically not sensitive to SD interactions as on the contrary ^{23}Na and ^{127}I are. Therefore, first model dependent analyses of the data have been performed by considering a candidate in this scenario, that is neglecting the term $\left(\frac{d\sigma}{dE_R}\right)_{SD}$ in eq. (1).

A full energy and time correlation analysis – properly accounting for the physical constraint arising from the measured upper limit on recoils [22, 30] – has been carried out in the framework of a given model for spin-independent coupled candidates with mass above 30 GeV. A standard maximum likelihood method has been used*. Following the usual procedure we have built the y log-likelihood function, which depends on the experimental data and on the theoretical expectations; then, y is minimized and parameters' regions allowed at given confidence level are derived. Note that different model frameworks (see above) vary the expectations and, therefore, the cross section and mass values corresponding to the y minimum, that is also the allowed region at given C.L.. In particular, the inclusion of the uncertainties associated to the models and to every parameter in the models themselves as well as other possible scenarios enlarges the allowed region as discussed e.g. in ref. [28] for the particular case of the astrophysical velocities. Also in the case considered here the minimization procedure has been repeated by varying the WIMP local velocity, v_0, from 170 km/s to 270 km/s to account for its present uncertainty. For

*Substantially the same results are obtained with other analysis approaches such as e.g. the Feldman and Cousins one.

example, in the model framework considered in ref. [29], the values $m_W = (72^{+18}_{-15})$ GeV and $\xi\sigma_{SI} = (5.7 \pm 1.1) \cdot 10^{-6}$ pb correspond to the position of y minimum when $v_0 = 170$ km/s, while $m_W = (43^{+12}_{-9})$ GeV and $\xi\sigma_{SI} = (5.4 \pm 1.0) \cdot 10^{-6}$ pb when $v_0 = 220$ km/s. Here, ξ is the WIMP local density in 0.3 GeV cm^{-3} unit, σ_{SI} is the point-like SI WIMP-nucleon generalized cross section and m_W is the WIMP mass. Fig. 6 shows the regions allowed at 3σ C.L. in such a model framework, when the uncertainty on v_0 is taken into account (solid contour) and when possible bulk halo rotation is considered (dashed contour). For simplicity, no other uncertainties on the used parameters have been considered there (some of them have been included in the approach summarized in the next subsection [31]), which obviously further enlarge the allowed region with the respect both to $\xi\sigma_{SI}$ and m_W.

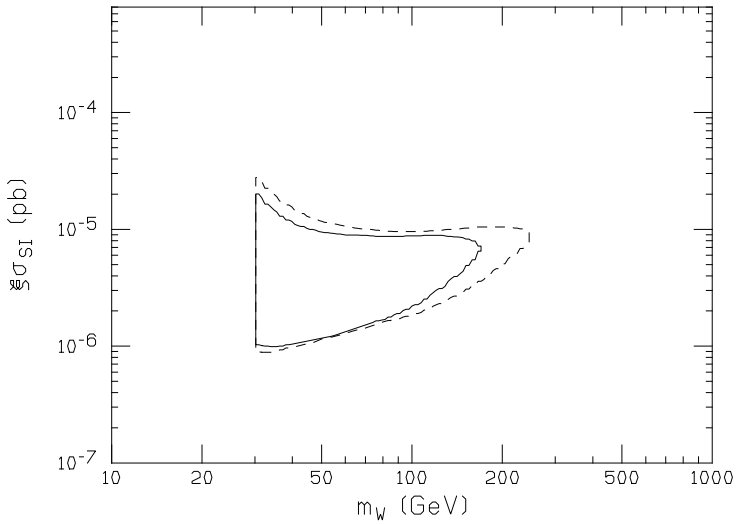

Figure 6: Regions allowed at 3σ C.L. on the plane $\xi\sigma_{SI}$ versus m_W for a WIMP with dominant SI interaction and mass above 30 GeV in the model framework considered in ref. [29]: i) when v_0 uncertainty (170 km/s $\leq v_0 \leq$ 270 km/s; continuous contour) has been included; ii) when also a possible bulk halo rotation as in ref. [28] (dashed contour) is considered. As widely known, the inclusion of present uncertainties on some other astrophysical, nuclear and particle physics parameters would enlarge these regions (varying consequently the position of the minimum for the y log-likelihood function).

A quantitative comparison between the results of the model independent analysis and of this model dependent analysis has been discussed in ref. [29].

In conclusion, the observed effect investigated in terms of a WIMP candidate with dominant SI interaction and mass above 30 GeV in the model framework considered in ref. [29], supports allowed WIMP masses up to 130 GeV (1 σ C.L.) and even up to 180 GeV (1 σ C.L.) if possible dark halo rotation is included, while lower $\xi\sigma_{SI}$ would be implied by the inclusion of known uncertainties on parameters (for example, on the form factor parameters) and model features.

Theoretical implications of these results in terms of a neutralino with dominant SI

interaction and mass above 30 GeV have been discussed in ref. [33, 34, 35], while the case for an heavy neutrino of the fourth family has been considered in ref. [36].

II. WIMPs with mixed coupling in given model framework

Since the ^{23}Na and ^{127}I nuclei are sensitive to both SI and SD couplings – on the contrary e.g. of ^{nat}Ge and ^{nat}Si which are sensitive mainly to WIMPs with SI coupling (only 7.8 % is non-zero spin isotope in ^{nat}Ge and only 4.7% of ^{29}Si in ^{nat}Si) – the analysis of the data has been extended considering the more general case of eq. (1) [31]. This implies a WIMP having not only a spin-independent, but also a spin-dependent coupling different from zero, as it is also possible e.g. for the neutralino (see above).

Following the usual procedure we have built the y log-likelihood function, which depends on the experimental data and on the theoretical expectations in the given model framework. Then, y has been minimized – properly accounting also for the physical constraint set by the measured upper limit on recoils [22] – and parameters' regions allowed at given confidence level have been obtained. In particular, the calculation has been performed by minimizing the y function with respect to the $\xi\sigma_{SI}$, $\xi\sigma_{SD}$ and m_W parameters for each given θ value. Here, σ_{SD} is the point-like SD WIMP cross section on nucleon and $tg\theta$ is the ratio between the effective SD coupling constants on neutrons, a_n, and on proton, a_p; therefore, θ can assume values between 0 and π depending on the SD coupling. In the present framework the uncertainties on v_0 have been included; moreover, the uncertainties on the nuclear radius and the nuclear surface thickness parameter in the SI form factor, on the b parameter in the used SD form factor (see later) and on the measured quenching factors [22] of these detectors have also been considered [31].

Fig. 7 shows slices for some m_W of the region allowed at 3 σ C.L. in the ($\xi\sigma_{SI}$, $\xi\sigma_{SD}$, m_W) space for some θ value. Only the case of four particular couplings are shown here for simplicity: i) $\theta = 0$ (a_n =0 and $a_p \neq 0$ or $|a_p| >> |a_n|$); ii) $\theta = \pi/4$ ($a_p = a_n$); iii) $\theta = \pi/2$ ($a_n \neq 0$ and $a_p = 0$ or $|a_n| >> |a_p|$); iv) $\theta = 2.435$ rad ($\frac{a_n}{a_p}$ = -0.85, pure Z^0 coupling). The case $a_p = -a_n$ is nearly similar to the case iv).

Comments about other discussions of purely SD component as well as about the comparisons with other direct and indirect experiments can be found in ref. [31].

As already pointed out, when the SD contribution goes to zero (y axis in Fig. 7), an interval not compatible with zero is obtained for $\xi\sigma_{SI}$. Similarly, when the SI contribution goes to zero (x axis in Fig. 7), finite values for the SD cross section are obtained. Large regions are allowed for mixed configurations also for $\xi\sigma_{SI} \lesssim 10^{-5}$ pb and $\xi\sigma_{SD} \lesssim 1$ pb; only in the particular case of $\theta = \frac{\pi}{2}$ (that is $a_p = 0$ and $a_n \neq 0$) $\xi\sigma_{SD}$ can increase up to $\simeq$ 10 pb, since the ^{23}Na and ^{127}I nuclei have the proton as odd nucleon. Moreover, in ref. [31] we have also pointed out that: i) finite values can be allowed for $\xi\sigma_{SD}$ even when $\xi\sigma_{SI} \simeq 3 \cdot 10^{-6}$ pb as in the region allowed in the pure SI scenario considered in the previous subsection; ii) regions not compatible with zero in the $\xi\sigma_{SD}$ versus m$_W$ plane are allowed even when $\xi\sigma_{SI}$ values much lower than those allowed in the dominant SI scenario previously summarized are considered; iii) minima of the y function with both $\xi\sigma_{SI}$ and

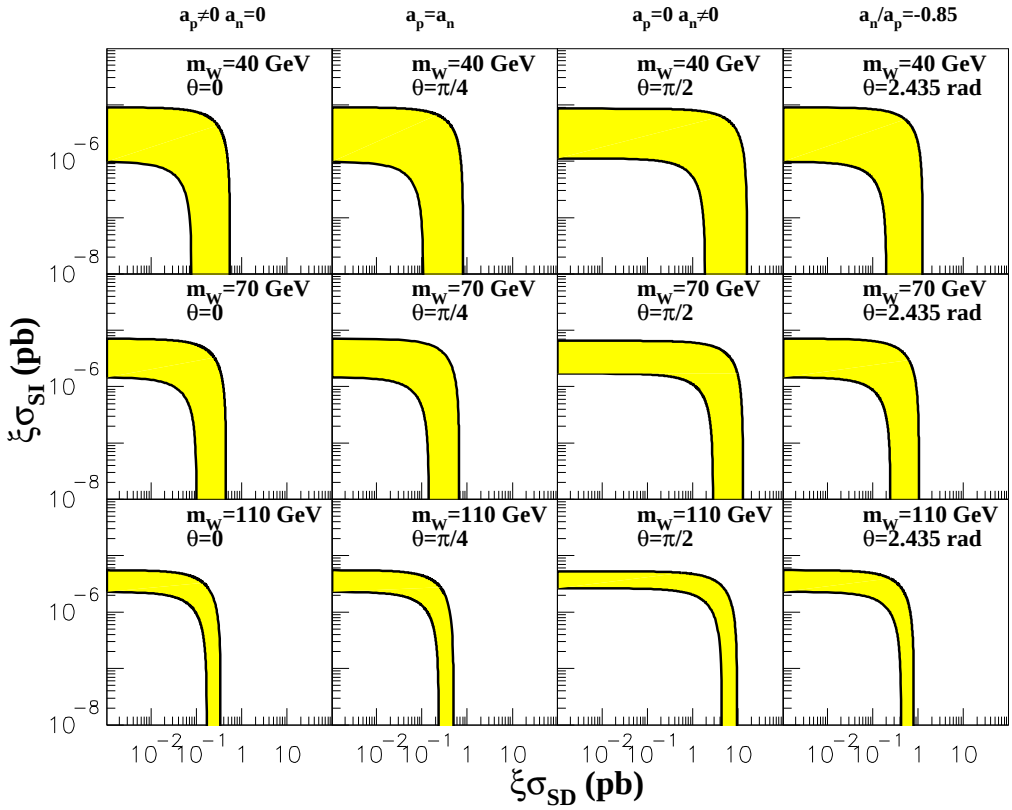

Figure 7: Slices for some m_W of the region allowed at 3 σ C.L. in the ($\xi\sigma_{SI}$, $\xi\sigma_{SD}$, m_W) space for some θ value in the model framework considered in ref. [31]. Only four particular couplings are reported here for simplicity: i) $\theta = 0$; ii) $\theta = \pi/4$ iii) $\theta = \pi/2$; iv) $\theta = 2.435$ rad.

$\xi\sigma_{SD}$ different from zero are present for some m_W and θ pairs; the related confidence level ranges between $\simeq 3$ σ and $\simeq 4$ σ [31].

In conclusion, this analysis has shown that the DAMA data of the four annual cycles, analysed in terms of WIMP annual modulation signature, can also be compatible with a mixed scenario where both $\xi\sigma_{SI}$ and $\xi\sigma_{SD}$ are different from zero. The pure SD and pure SI cases in the model framework considered here are implicitly given in Fig. 7 for the quoted m_W and θ values.

Further investigations are in progress on these model dependent analyses to account for other known parameters uncertainties and for possible different model assumptions. As an example we recall that for the SD form factor an universal formulation is not possible since the internal degrees of the WIMP particle model (e.g. supersymmetry in case of neutralino) cannot be completely separated from the nuclear ones. In the calculations presented here we have adopted the SD form factors of ref. [37] estimated by considering the Nijmengen nucleon-nucleon potential. Other formulations are possible for SD form factors and can be considered with evident implications on the obtained allowed regions.

III. Inelastic Dark matter

It has been recently suggested [38] the possibility that the observed annual modulation of the low energy rate could be induced by possible inelastic Dark Matter: relic particles that cannot scatter elastically off of nuclei. As discussed in ref. [38], the inelastic Dark Matter could arise from a massive complex scalar split into two approximately degenerate real scalars or from a Dirac fermion split into two approximately degenerate Majorana fermions, namely χ_+ and χ_-, with a δ mass splitting. In particular, a specific model featuring a real component of the sneutrino, in which the mass splitting naturally arises, has been given in ref. [38]. It has been shown that for the χ_- inelastic scattering on target nuclei a kinematical constraint exists which favours heavy nuclei (such as ^{127}I) with respect to lighter ones (such as e.g. ^{nat}Ge) as target-detectors media. In fact, χ_- can only inelastically scatter by transitioning to χ_+ (slightly heavier state than χ_-) and this process can occur only if the χ_- velocity, v, is larger than:

$$v_{thr} = \sqrt{\frac{2\delta}{m_{WN}}}, \tag{2}$$

where m_{WN} is the WIMP-nucleus reduced mass and hereafter $c = 1$. This kinematical constraint becomes increasingly severe as the nucleus mass, m_N, is decreased [38]. Moreover, this model scenario gives rise – with respect to the case of WIMP elastically scattering – to an enhanced modulated component, S_m, with respect to the unmodulated one, S_0, and to largely different behaviours with energy for both S_0 and S_m (both show a higher mean value) [38].

For the sake of completeness, we remind that – as stressed in ref. [38] – this scenario is suitable to reconcile in every case the DAMA result [26, 27, 28, 29, 30, 31, 32] with the CDMS-I claim [39]; however, it is worth to note that – as discussed e.g. in sect. III of ref. [40] – in reality the claim for contradiction made by CDMS-I was largely unjustified both for experimental and theoretical reasons.

Anyhow, the proposed inelastic Dark Matter scenario [38] offers a further possible model framework, which has also the merit to recover the sneutrino as a suitable WIMP candidate.

Therefore, a dedicated energy and time correlation analysis of the DAMA experimental data has been carried out [32] by considering the data collected during four annual cycles (statistics of 57986 $kg \times day$) [26, 27, 28, 29, 30, 31, 32]. Here aspects other than the interaction type have been handled according to ref. [31], fixing in this way a given model framework.

In this inelastic Dark Matter scenario an allowed volume in the space ($\xi\sigma_p$,m_W,δ) is obtained [32]. For simplicity, Fig. 8 shows slices of such an allowed volume at some given WIMP masses (3 σ C.L.). It can be noted that when $m_W \gg m_N$, the expected differential energy spectrum is trivially dependent on m_W and in particular it is proportional to the ratio between $\xi\sigma_p$ and m_W; this particular case is summarized in the last plot of Fig. 8. The allowed regions reported there have been obtained by the superposition of those

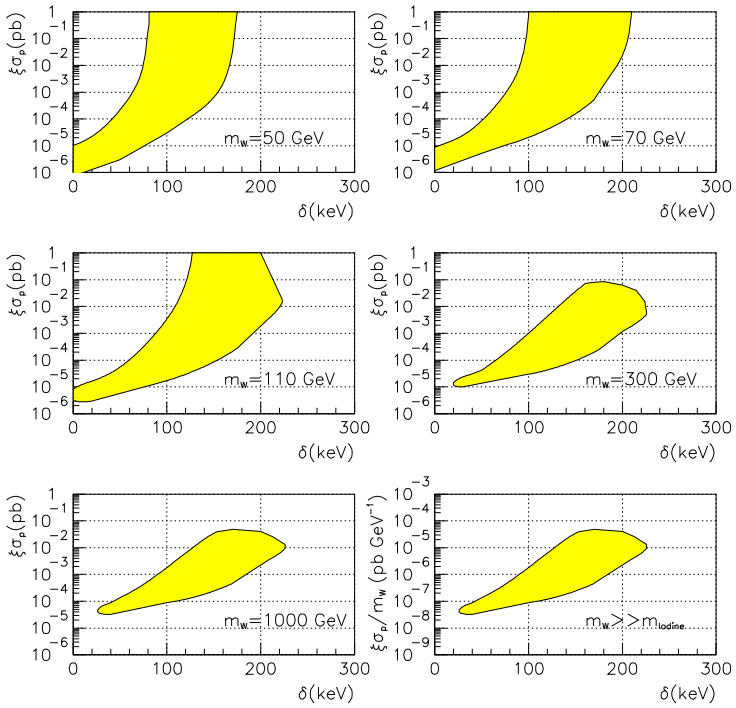

Figure 8: Slices at fixed WIMP masses of the volume allowed at 3 σ C.L. in the space ($\xi\sigma_p$, δ, m_W); the uncertainties on some of the used parameters have been included [32]. See text.

obtained when varying the values of the previously mentioned parameters according to their uncertainties. This also gives as a consequence that the cross section value at given δ can span there over several orders of magnitude. The upper border of each region is reached when v_{thr} approximates the maximum WIMP velocity in the Earth frame for each considered model framework (in particular, for each v_0 value).

Note that each set of values (within those allowed by the associated uncertainties) for the previously mentioned parameters gives rise to a different expectation, thus to different best fit values. As an example we mention that when fixing the other parameters as in Ref. [31], the best-fit values for a WIMP mass of 70 GeV are: i) $\xi\sigma_p = 2.5 \times 10^{-2}$ pb and $\delta = 115$ keV when $v_0 = 170$ km/s, ii) $\xi\sigma_p = 6.3 \times 10^{-4}$ pb and $\delta = 122$ keV when $v_0 = 220$ km/s.

Finally, we note also here that significant enlargement of the given allowed regions should be expected when including complete effects of model (and related experimental and theoretical parameters) uncertainties. Moreover, possible different halo models can be also considered.

6.3 Conclusions

The DAMA annual modulation data of four annual cycles [26, 27, 28, 29, 30, 31, 32] have been analysed by energy and time correlation analysis in terms of purely SI, purely SD, mixed SI/SD, "preferred" inelastic WIMP scattering model frameworks.

To effectively discriminate among the different possible scenarios further investigations are in progress. In particular, the data of the 5^{th} and 6^{th} annual cycles are at hand, while the set-up is running to collect the data of a 7^{th} annual cycle. Moreover, the LIBRA (Large sodium Iodine Bulk for RAre processes) set-up is under construction to increase the experimental sensitivity.

7 Towards LIBRA

At present our main efforts are devoted to the realization of LIBRA (Large sodium Iodine Bulk for RAre processes in the DAMA experiment) consisting of $\simeq$ 250 kg of NaI(Tl). New radiopure detectors by chemical/physical purification of NaI and Tl powders as a result of a dedicated R&D with Crismatec have been realized. This will allow to increase the sensitivity of the experiment.

References

[1] P. Belli et al., *Astrop. Phys.* 5 (1996) 217.

[2] R. Bernabei et al., *Il Nuovo Cimento* A110 (1997) 189.

[3] R. Bernabei et al., *Phys. Lett.* B408 (1997) 439.

[4] R. Bernabei et al., *Astrop. Phys.* 7 (1997) 73.

[5] P. Belli et al., *Nucl. Phys.* B563 (1999) 97.

[6] P. Belli et al., *Astrop. Phys.* 10 (1999) 115.

[7] P. Belli et al., *Phys. Rev.* C60 (1999) 065501.

[8] P. Belli et al., *Phys. Lett.* B460 (1999) 236.

[9] P. Belli et al., *Phys. Lett.* B 465 (1999) 315.

[10] P. Belli et al., *Phys. Rev.* D 61 (2000) 117301.

[11] R. Bernabei et al., *Phys. Lett.* B 493 (2000) 12.

[12] R. Bernabei et al., *Phys. Lett.* B515 (2001) 6.

[13] R. Bernabei et al., IFNF/AE-01/19 available as on-line pre-print at www.lngs.infn.it, submitted for publication.

[14] P. Belli et al., *Il Nuovo Cimento* A 103 (1990) 767.

[15] P. Belli et al., *Nucl. Instr. & Methods* A 316 (1992) 55; *Nucl. Instr. & Methods* A 336 (1993) 36; *Nucl. Phys.* B (Proc. Sup.) 35 (1993) 165; *Proc. The Dark side of the Universe*, World Sc. (1993) 257; *Proc. The Dark side of the Universe*, World Sc. (1995) 177; *Proc. ICRC95* vol.II (1995) 865.

[16] R. Bernabei et al., ROM2F/2001-09 and IFNF/AE-01/02 available as on-line pre-print at www.lngs.infn.it, to appear on *Nucl. Instr. & Meth.* A.

[17] P. Belli et al., *Il Nuovo Cimento* C 19 (1996) 537.

[18] P. Belli et al., *Phys. Lett.* B 387 (1996) 222; *Phys. Lett.* B 389 (1996) 783(err.).

[19] R. Bernabei et al., *Phys. Lett.* B 436 (1998) 379.

[20] R. Bernabei et al., *New Journal of Physics* 2 (2000) 15.1-15.7, (www.njp.org).

[21] R. Bernabei et al., *Eur. Phys. J. direct* C11 (2001) 1.

[22] R. Bernabei et al., *Phys. Lett.* B389 (1996) 757.

[23] R. Bernabei et al., *Il Nuovo Cimento* A112 (1999) 1541.

[24] R. Bernabei et al., *Phys. Rev. Lett.* 83 (1999) 4918.

[25] R. Bernabei et al., *Il Nuovo Cimento* A112 (1999) 545.

[26] R. Bernabei et al., *Phys. Lett.* B424 (1998) 195.

[27] R. Bernabei et al., *Phys. Lett.* B450 (1999) 448.

[28] P. Belli et al., *Phys. Rev.* D61 (2000) 023512.

[29] R. Bernabei et al., *Phys. Lett.* B480 (2000) 23.

[30] R. Bernabei et al., *Eur. Phys. J.* C18 (2000) 283.

[31] R. Bernabei et al., *Phys. Lett.* B509 (2001) 197.

[32] R. Bernabei el al., ROM2F/2001/33, to appear on *Eur. Phys. J.* C.

[33] A. Bottino et al., *Phys. Lett.* B402 (1997) 113; *Phys. Lett.* B423 (1998) 109; *Phys. Rev.* D59 (1999) 095004; *Phys. Rev.* D59 (1999) 095003; *Astrop. Phys.* 10 (1999) 203; *Astrop. Phys.* 13 (2000) 215; *Phys. Rev.* D62 (2000) 056006; hep-ph/0010203; hep-ph/0012377.

[34] A. Bottino et al., *Phys. Rev.* D62 (2000) 056006.

[35] R.W. Arnowitt and P. Nath, *Phys. Rev.* D60 (1999) 044002; E. Gabrielli et al., hep-ph/0006266.

[36] D. Fargion et al., *Pis'ma Zh. Eksp. Teor. Fiz.* 68, (*JETP Lett.* 68, 685) (1998); *Astrop. Phys.* 12 (2000) 307.

[37] M.T. Ressell et al., *Phys. Rev.* C56 (1997) 535.

[38] D. Smith and N. Weiner, *Phys. Rev.* D64 (2001) 043502.

[39] CDMS collaboration, *Phys. Rev. Lett.* 84 (2000) 5699.

[40] P. Belli et al., in the volume "Relativistic Astrophysics", 20th Texas Symp., AIP (2001) 95; pre-print available on DAMA homepage on http://www.lngs.infn.it.